

Study of relaxation oscillations in continuous-wave intracavity Raman lasers

Jipeng Lin*, Helen M. Pask, Andrew J. Lee, and David J. Spence

MQ Photonics Research Centre, Department of Physics and Engineering, Macquarie University, NSW 2109 Australia

**Jipeng@science.mq.edu.au*

Abstract: We study the relaxation oscillations in a continuous-wave intracavity Raman laser both theoretically and experimentally. Analytic expressions for the relaxation oscillation frequency are derived from the rate-equations and are validated by experiments. We show that some important experimental parameters such as the effective Raman gain coefficient and intracavity Stokes loss can be determined simply by measuring the relaxation oscillation frequency versus pump power.

©2010 Optical Society of America

OCIS codes: (140.3550) Lasers, Raman; (140.3480) Lasers, diode-pumped; (190.2620) Nonlinear optics, harmonic generation and mixing.

References and links

1. A. A. Demidovich, A. S. Grabchikov, V. A. Lisinetskii, V. N. Burakevich, V. A. Orlovich, and W. Kiefer, "Continuous-wave Raman generation in a diode-pumped Nd³⁺:KGd(WO₄)₂ laser," *Opt. Lett.* **30**(13), 1701–1703 (2005).
2. H. M. Pask, "Continuous-wave, all-solid-state, intracavity Raman laser," *Opt. Lett.* **30**(18), 2454–2456 (2005).
3. L. Fan, Y. X. Fan, Y. Q. Li, H. J. Zhang, Q. Wang, J. Wang, and H. T. Wang, "High-efficiency continuous-wave Raman conversion with a BaWO₄ Raman crystal," *Opt. Lett.* **34**(11), 1687–1689 (2009).
4. A. J. Lee, H. M. Pask, P. Dekker, and J. A. Piper, "High efficiency, multi-Watt CW yellow emission from an intracavity-doubled self-Raman laser using Nd:GdVO₄," *Opt. Express* **16**(26), 21958–21963 (2008).
5. D. J. Spence, P. Dekker, and H. M. Pask, "Modeling of continuous wave intracavity Raman lasers," *IEEE J. Sel. Top. Quantum Electron.* **13**(3), 756–763 (2007).
6. D. C. Hanna, D. J. Pointer, and D. J. Pratt, "Stimulated Raman scattering of picosecond light pulses in hydrogen, deuterium, and Methane," *IEEE J. Quantum Electron.* **22**(2), 332–336 (1986).
7. P. Cerný, H. Jelinkova, P. G. Zverev, and T. T. Basiev, "Solid state lasers with Raman frequency conversion," *Prog. Quantum Electron.* **28**(2), 113–143 (2004).
8. T. T. Basiev, A. A. Sobol, P. G. Zverev, V. V. Osiko, and R. C. Powell, "Comparative spontaneous Raman spectroscopy of crystals for Raman lasers," *Appl. Opt.* **38**(3), 594–598 (1999).
9. A. A. Kaminskii, H. J. Eichler, K. Ueda, N. V. Klassen, B. S. Redkin, L. E. Li, J. Findeisen, D. Jaque, J. García-Sole, J. Fernández, and R. Balda, "Properties of Nd³⁺-doped and undoped tetragonal PbWO₄, NaY(WO₄)₂, CaWO₄, and undoped monoclinic ZnWO₄ and CdWO₄ as laser-active and stimulated Raman scattering-active crystals," *Appl. Opt.* **38**(21), 4533–4547 (1999).
10. S. Ding, X. Zhang, Q. Wang, F. Su, P. Jia, S. Li, S. Li, S. Fan, J. Chang, S. Zhang, and Z. Liu, "Theoretical and experimental study on the self-Raman laser with Nd:YVO₄ crystal," *IEEE J. Quantum Electron.* **22**, 927–933 (2006).
11. D. Findlay, and R. A. Clay, "The measurement of internal losses in 4-level lasers," *Phys. Lett.* **20**(3), 277–278 (1966).
12. J. A. Caird, S. A. Payne, P. R. Staber, A. J. Ramponi, L. L. Chase, and W. F. Krupke, "Quantum electronic properties of the Na₃Ga₂Li₃F₁₂: Cr³⁺ Laser," *IEEE J. Quantum Electron.* **24**(6), 1077–1099 (1988).
13. A. E. Siegman, *Lasers* (University Science Books, Mill Valley, Calif. 1986) Chap. 25, pp. 962–964; Chap. 11, pp. 428–429.
14. K. J. Weingarten, B. Braun, and U. Keller, "In situ small-signal gain of solid-state lasers determined from relaxation oscillation frequency measurements," *Opt. Lett.* **19**(15), 1140–1142 (1994).
15. D. C. Hanna, R. G. Smart, P. J. Suni, A. I. Ferguson, and M. W. Phillips, "Measurements of fibre laser losses via relaxation oscillations," *Opt. Commun.* **68**(2), 128–132 (1988).
16. A. A. Kaminskii, K. Ueda, H. J. Eichler, Y. Kuwano, H. Kouta, S. N. Bagaev, T. H. Chyba, J. C. Barnes, G. M. A. Gad, T. Murai, and J. R. Lu, "Tetragonal vanadates YVO₄ and GdVO₄ - new efficient χ (3)-materials for Raman lasers," *Opt. Commun.* **194**(1-3), 201–206 (2001).

1. Introduction

The first continuous-wave (CW) intracavity crystalline Raman lasers, reported in 2005 [1,2], have attracted considerable attention due to their capability to access to the spectral region between 1.1 and 1.5 μm . By further incorporating intracavity frequency-doubling, the yellow and orange spectral region can also be accessed; laser wavelengths in this region are of considerable interest for applications in defense, atmospheric science, biomedical diagnostics, and laser therapies. Power output from crystalline CW Raman lasers has exceeded 3 W in the near infrared [3] and over 2.5 W in the yellow [4].

In the development of high power, efficient CW intracavity crystalline Raman lasers, the steady-state Raman gain coefficient g_R and the intracavity losses, δ_F and δ_S , for the fundamental and Stokes optical fields respectively, are important design parameters, influencing both Raman threshold and overall efficiency [5]. By using a Raman crystal with higher g_R or by reducing δ_F and δ_S , the laser system has reduced threshold and higher efficiency.

One method to determine g_R for Raman crystals is to measure the stimulated Raman scattering (SRS) threshold for a Raman medium pumped by a high intensity pulsed laser [6,7]. Another approach [8,9] is to compare the peak scattering intensity Σ_{peak} in the spontaneous Raman spectrum of the Raman crystal sample with that of a reference Raman crystal (e.g. diamond, BN, or KGW) whose g_R is known. These conventional methods are not convenient for in situ measurement and are specific to the excitation wavelength used. Moreover, in an intracavity Raman laser system in which the Stokes field perturbs the fundamental field, the effective Raman gain g_R^{eff} that governs the power flow between them is usually less than g_R due to transverse effects, causing discrepancies between modeling and experimental results [10]. To characterize and optimize the performance of such a Raman laser system, it is important to know this effective g_R .

To determine cavity loss δ_F for a classical four-level laser, one can measure the laser threshold and slope efficiency with several different output couplers and apply the Findlay-Clay or Caird analysis [11,12]. However, these methods are unpractical in the context of a CW intracavity Raman laser for which the output coupler coating has more complex requirements, namely high reflectivity at the fundamental and typically 0.5-2% output coupling at the Stokes wavelength. Another method of determining δ_F for a fundamental laser is to measure the relaxation oscillation frequency (ROF) as a function of pump power [13], a method which has been widely used when characterizing solid-state lasers [14] and fiber lasers [15]. The theory and application of the ROF method to a CW intracavity Raman laser has not been reported previously.

In this paper, we present a rate-equation analysis for predicting the ROF in a CW intracavity Raman laser. We derive the analytic expressions of ROF as a function of pump power P , and show that both g_R^{eff} and Stokes cavity loss δ_S can be determined simply by measuring the ROF versus pump power below and above the Raman threshold. We then experimentally verify this theory by constructing a CW intracavity self-Raman laser based on Nd:GdVO₄ and comparing our experimentally-determined values of g_R^{eff} with values for g_R found in the literature. We anticipate this method may be useful in selection and evaluation of Raman crystals and cavity designs to optimize the performance of a CW Raman laser.

2. Theory

We consider a CW intracavity Raman laser (typical set up is shown in Fig. 1) with a laser crystal pumped by a laser-diode (LD), and a Raman crystal. The theory can also be applied to a CW intracavity self-Raman laser that utilises a single crystal such as Nd:GdVO₄, Nd:YVO₄ or Nd:KGW as both the laser and Raman material. The resonator is formed by an input mirror M1 and an output coupler M2. M1 has a high-reflectivity (HR) coating for both fundamental and first-Stokes wavelengths, and high-transmission (HT) coating for the pump wavelength,

while M2 has a HR coating for fundamental wavelength and a transmission of T_R for the first-Stokes wavelength.

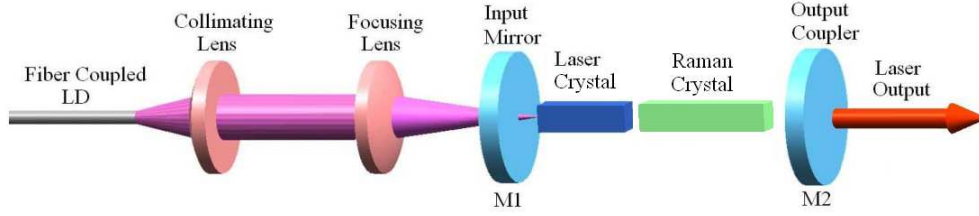


Fig. 1. Schematic diagram of a CW intracavity Raman laser.

As the diode pump power is increased, threshold for lasing at the fundamental is exceeded. The expression describing the ROF ω for fundamental laser is given by [13]:

$$\omega^2 = k_f P - b_f \quad (1)$$

$$k_f = AC; \quad b_f = \frac{1}{\tau\tau_f}; \quad A = \frac{\lambda_p}{hcV}; \quad C = \frac{c\sigma l_c}{L}$$

Here L is the optical cavity length, l_c is the length of laser crystal, σ , τ are the laser crystal emission cross section and the upper-laser level lifetime, P is the absorbed pump power, τ_f is the fundamental cavity decay time, λ_p is the wavelength of the LD, and V is the pumped volume in the laser crystal.

As more pump power is absorbed in the laser crystal, the fundamental intracavity intensity increases and reaches the threshold for stimulated Raman scattering. Time-dependent rate-equations can describe the interplay among the fundamental and first Stokes intracavity intensities and the inversion in the laser crystal:

$$\begin{aligned} \frac{dN}{dt} &= AP - BNI_F - \frac{N}{\tau} \\ \frac{dI_F}{dt} &= CNI_F - DI_F I_S - \frac{I_F}{\tau_f} \\ \frac{dI_S}{dt} &= EI_F I_S - \frac{I_S}{\tau_s} \end{aligned} \quad (2)$$

$$B = \frac{2\lambda_f \sigma}{hc}; \quad D = \frac{2cg_R l_R \lambda_S A_L}{L\lambda_f A_R}; \quad E = \frac{2cg_R l_R A_L}{LA_R}$$

where N is the laser crystal inversion density, I_F , I_S are the fundamental and Stokes intracavity intensities in the laser crystal respectively, l_R is the length of Raman crystals, g_R is the stimulated Raman gain coefficient, τ_s is the Stokes cavity decay time, λ_f , λ_s are the wavelengths of the fundamental and Stokes respectively, A_L and A_R are the fundamental laser mode areas in the laser and Raman crystals respectively. For the special case of a self-Raman laser, $A_L = A_R$.

We now look for relaxation oscillation solutions to these equations that have the form of small oscillations around the equilibrium values. We assume that all three variables N , I_F , I_S consist of steady-state values N_0 , I_{F0} , I_{S0} and small offsets ΔN , ΔI_F , ΔI_S from the steady-state values:

$$N = N_0 + \Delta N; \quad I_F = I_{F0} + \Delta I_F; \quad I_S = I_{S0} + \Delta I_S \quad (3)$$

N_0, I_{F0}, I_{S0} can be obtained by setting each expression in Eq. (2) to zero. Here we make the approximation that $(B\tau + E\tau_S) \approx B\tau$ on the basis that $\tau \gg \tau_S$ and $E \approx B$. Numerical evaluation shows the error introduced by this is $<0.2\%$. We find the following steady-state values:

$$N_0 \approx \frac{AEP\tau_S}{B}; \quad I_{F0} = \frac{1}{E\tau_S}; \quad I_{S0} \approx \frac{1}{D} \left(\frac{ACEP\tau_S}{B} - \frac{1}{\tau_F} \right) \quad (4)$$

The Raman threshold P_{th} can be obtain by setting $I_{S0} = 0$:

$$P_{th} = \frac{\delta_F \delta_S A_R \lambda_F}{4g_R l_R \lambda_p} \quad (5)$$

The intracavity loss for fundamental and Stokes δ_F, δ_S includes the round-trip loss and the transmission of cavity mirrors.

By substituting Eq. (3) into Eq. (2), the derivatives of $\Delta N, \Delta I_F, \Delta I_S$ with respect to t are:

$$\begin{aligned} \frac{d\Delta N}{dt} &= -\Delta N \left(BI_{F0} + \frac{1}{\tau} \right) - \Delta I_F B N_0 \\ \frac{d\Delta I_F}{dt} &= CI_{F0} \Delta N - DI_{F0} \Delta I_S \\ \frac{d\Delta I_S}{dt} &= EI_{S0} \Delta I_F \end{aligned} \quad (6)$$

We now look for solutions of the form $\exp(pt)$ for $\Delta N, \Delta I_F$ and ΔI_S . From Eq. (6), we can obtain a cubic equation in p :

$$\begin{aligned} p^3 + Gp^2 + I_{F0}(CBN_0 + DEI_{S0})p + GDEI_{F0}I_{S0} &= 0 \\ G &= BI_{F0} + \frac{1}{\tau} \end{aligned} \quad (7)$$

From Eq. (7), p has a real solution $p = a$ corresponding to a simple decay of the offsets, and two conjugated complex solutions $p = -1/t_0 \pm i\omega$ describing the decaying relaxation oscillations that we are seeking, where t_0 is the envelope decay time, and ω is the ROF. An analytic expression for ω can be derived by making approximations that $\omega \gg 1/t_0$ and $\omega \gg a$, an assumption which introduces a small error of $\sim 0.15\%$:

$$\begin{aligned} \omega^2 &= k_S P - b_S \\ k_S &\approx AC \left(1 + \frac{E}{B} \right); \quad b_S = \frac{1}{\tau_F \tau_S} \end{aligned} \quad (8)$$

These equations now fully characterize the relaxation oscillations in a CW intracavity Raman laser. Using the known crystal and cavity parameters along with experimental measurements of the ROF below and above Raman threshold, we can determine g_R^{eff} and δ_S . If we plot ROF against pump power and make fits below and above the Raman threshold, the slope, k_S , above the Raman threshold divided by the slope, k_F , below the Raman threshold is equal to $(1 + E/B)$, from which we can then determine the effective Raman gain coefficient:

$$g_R^{eff} = \frac{\lambda_F \sigma L}{hc^2 l_R} \left(\frac{k_S}{k_F} - 1 \right) = \eta g_R \quad (9)$$

This effective Raman gain coefficient will be less than or equal to the material gain coefficient, by a transverse correction factor η , that can be determined by an integration of the intensity rate equations over the normalized transverse profiles of the parameters N, I_F , and I_S [10]. If the parameters have matched Gaussian profiles then the correction factor is in fact unity, and the intensity rate equations may be used uncorrected. However, if the beam sizes are not matched, or if the transverse profiles are not Gaussian, η will be less than one, and the effective gain averaged over the transverse dimensions will be reduced. Determination of g_R^{eff}

is important for two reasons. Firstly, we can in principle determine η and then calculate the material gain coefficient g_R . Secondly, we can use g_R^{eff} as a tool to evaluate the laser design with a view to maximizing the power flow between the fundamental and Stokes optical fields.

The ratio of the y-axis intercept b_S for the linear fit above the Raman threshold, to the intercept b_F for that below the Raman threshold is τ/τ_S , and from this quantity, the intracavity Stokes loss factor δ_S (which is independent of η) can be determined:

$$\delta_S = \frac{c}{2L\tau} \frac{b_S}{b_F} \quad (10)$$

3. Experiment

3.1 Experimental arrangement

We constructed a Raman laser to validate this method of measuring the Raman gain and cavity losses. We used a self-Raman laser configuration, in which the laser crystal is Raman-active, thereby serving the dual functions of generating the laser fundamental and Raman shifting to the first Stokes. The arrangement is similar to that shown in Fig. 1, except that only one crystal is used. To match the pump and fundamental mode areas, a high brightness 30 W 880 nm LD (LIMO $\Phi \sim 200 \mu\text{m}$, N.A. ~ 0.22 , unpolarized) was imaged into the AR-coated (1064 nm – 1200 nm) a-cut 0.3 at.%. Nd:GdVO₄ crystal which was placed close to the input mirror. The pump spot's radius was $\sim 170 \mu\text{m}$. The polarizations of the fundamental and Stokes beams were along c-axis of Nd:GdVO₄ crystal. The overall optical length of the resonator was 80 mm. Filters were used to separate the residual fundamental (1064 nm) and Stokes (1173 nm) laser beams, and a Ge photodiode connected to a spectrum-analyzer (Tektronix-2792) was used to determine the ROF.

We measured the ROF ω as a function of absorbed diode pump power in three separate experiments that used two sets of cavity mirrors as detailed in Table 1, and two crystals of different lengths. In the first experiment, a 20 mm long Nd:GdVO₄ crystal with mirror set A was used; in the second, the same 20 mm long Nd:GdVO₄ crystal with mirror set B; and in the third, a 10 mm long Nd:GdVO₄ crystal with mirror set B. For both mirror sets, the input mirrors were flat while the output couplers were concave ($R = 300 \text{ mm}$). Both the 10 mm and 20 mm crystals had the same surface coating ($R < 0.1\%$ at 1064 nm - 1173 nm). The rationale of using these three experiments was to determine and compare the values of g_R^{eff} and δ_S by fixing at least one parameter (crystal length or cavity mirror set) between experiments.

Table 1. Reflectivity of the two sets of cavity mirrors at fundamental and Stokes wavelengths.

	Mirror Set A		Mirror Set B	
	λ_F	λ_S	λ_F	λ_S
M1: Reflectivity (%)	99.994	99.996	99.91	99.61
M2: Reflectivity (%)	99.91	99.61	99.91	99.61
Total transmission (%)	0.096	0.394	0.18	0.788

3.2 Results and discussions

Figure 2 shows the experimental results of ω^2 vs absorbed pump power both above and below the Raman threshold P_{th} in (a) 20 mm long crystal with two sets of mirrors; and (b) mirror set A with 10 mm and 20 mm long crystal. The abrupt change in slope occurs at the Raman threshold, above which the fundamental and the Stokes have the same ROF. The error for measuring the ROF is about $\pm 1.5\%$.

3.2.1 Raman gain coefficient g_R

The value of $g_R^{eff} l_R$ is proportional to $k_S/k_F - 1$, and was determined from Fig. 2. In Fig. 2(a), below Raman threshold the fit lines for both mirror sets nearly overlap due to similar fundamental laser performance. Above the threshold, the two fit lines are nearly parallel because of the similar value of $g_R^{eff} l_R$ using the same crystal length. In Fig. 2(b), below Raman threshold, k_F for the 10 mm crystal is slightly larger than that of 20 mm crystal due to slightly smaller pump volume V . The value of $k_S/k_F - 1$ of the 10 mm crystal is around half of that of the 20 mm crystal, which is consistent with the ratio of the length of the two crystals.

For the linear fits shown in Fig. 2, the calculated values for g_R^{eff} in our Raman laser system are 2.35 ± 0.10 cm/GW for 20 mm crystal with mirror set A, 2.42 ± 0.15 cm/GW for 20 mm crystal with mirror set B, and 2.46 ± 0.15 cm/GW for 10 mm crystal with mirror set A. The measurement errors ($\pm 3.0\%$ for k_S , $\pm 3.35\%$ for k_F) were quantified by its uncertainties in the linear fit to the experimental data with $\pm 1.5\%$ error determining the ROF.

The values for g_R^{eff} are similar for all three lasers, indicating similar values for η of order 0.5 in each case, using the reported value for g_R of 4.5 cm/GW [16]. Measurements of the transverse profiles in the laser showed that the beam radius of the fundamental was approximately twice that of the Stokes, with the fundamental field substantially suppressed on axis compared to a Gaussian profile. For *Gaussian* beams mismatched in this way we calculate $\eta = 0.77$, and we attribute the remaining reduction in the effective gain to the observed non-Gaussian profile of the fundamental beam. We note that achieving higher values of η is difficult in practice, since Raman beam cleanup usually leads to the beam quality of the Stokes being better than that of the fundamental, and at the same time stronger axial depletion of the fundamental by the Stokes tends to degrade the beam quality of the fundamental.

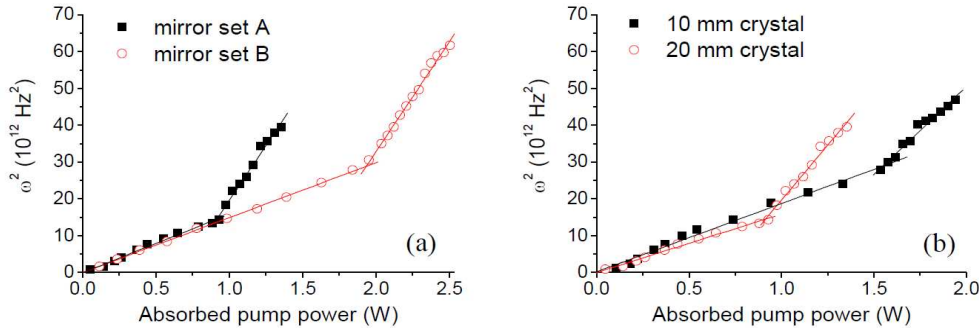


Fig. 2. Measured ω^2 vs absorbed pumped power in (a) 20 mm long crystal with mirror sets A and sets B; (b) 10 mm and 20 mm crystals with mirror set A. The error bar was $\pm 1.5\%$ for every point.

3.2.2 Intracavity Stokes loss, δ_S

The intracavity Stokes loss consists of the total mirror transmission losses (see Table 1) as well as losses associated with the Nd:GdVO₄ crystal, including the effect of AR-coating losses, surface and volume losses, and potentially linear or nonlinear losses associated with impurity absorption and upconversion. Each of these is difficult to quantify, particularly the effect of reflections from AR coatings, since some of these reflections re-enter the resonator mode.

We have calculated values for δ_S using Eq. (10) to be 0.562% for 20 mm crystal with mirror set A, 0.911% for 20 mm crystal with mirror set B, and 0.623% for 10 mm crystal with mirror set A. Taking into account that the total mirror transmission losses are 0.394%, 0.788% and 0.394% for the three experimental cases, we can infer overall losses associated with the crystal of $0.168 \pm 0.045\%$, $0.123 \pm 0.033\%$ and $0.229 \pm 0.061\%$, respectively. As already noted, the primary sources of error are from linear fit ($\pm 1.5\%$ for δ_S , $\pm 25\%$ for δ_F). We can

also calculate the overall fundamental loss associated with the crystal, using Eq. (8) and (10), to be $0.21 \pm 0.06\%$, $0.29 \pm 0.08\%$ and $0.185 \pm 0.049\%$ for three experiments respectively. The calculated overall losses for the same 20 mm crystal in the first and second experiments are equal to within the errors.

The measured Stokes losses are also consistent with the observed Raman thresholds, for which P_{th} which is proportional to the value of $\delta_S \delta_F / g_R l_R$. In Fig. 2(a) where the same self-Raman crystal is employed, the thresholds measured for mirror sets A and B were 0.92 W and 1.95 W respectively. The ratio of these is 2.12, which compares well with the calculated ratio of our measured $\delta_S \delta_F$ for the experiments using different mirror sets, which is 2.23.

4. Conclusions

We have calculated the behaviour of the relaxation oscillation frequency as a function of pump power for a CW intracavity Raman laser, and demonstrated a useful method to measure the effective Raman gain coefficient g_R^{eff} and intracavity loss factor of Stokes δ_S . This method is convenient as it enables an in situ determination of δ_S and g_R^{eff} for a given Raman laser system that can be applied to any intracavity Raman or self-Raman laser.